Nano Today 36 (2021) 101027

Contents lists available at ScienceDirect

Nano Today

journal homepage: www.elsevier.com/locate/nanotoday

Nanozyme scavenging ROS for prevention of pathologic α-synuclein transmission in Parkinson's disease

Yu-Qing Liu[a,1], Yuanyang Mao[b,1], Enquan Xu[c,d], Huimin Jia[b], Shu Zhang[c,d], Valina L. Dawson[c,d,e,f,h,i], Ted M. Dawson[c,d,e,g,h,i], Yan-Mei Li[a,**], Zhi Zheng[b,**], Weiwei He[b,**], Xiaobo Mao[c,d,*]

[a] Key Laboratory of Bioorganic Phosphorus Chemistry & Chemical Biology (Ministry of Education), Department of Chemistry, Tsinghua University, Beijing, 100084, China
[b] Key Laboratory of Micro-Nano Materials for Energy Storage and Conversion of Henan Province, Henan Joint International Research Laboratory of Nanomaterials for Energy and Catalysis, Institute of Surface Micro and Nano Materials, College of Chemical and Materials Engineering, Xuchang University, Xuchang, Henan, 461000, China
[c] Institute for Cell Engineering, Johns Hopkins University School of Medicine, Baltimore, MD, 21205, USA
[d] Department of Neurology, Johns Hopkins University School of Medicine, Baltimore, MD, 21205, USA
[e] Solomon H. Snyder Department of Neuroscience, Johns Hopkins University School of Medicine, Baltimore, MD, 21205, USA
[f] Department of Physiology, Johns Hopkins University School of Medicine, Baltimore, MD, 21205, USA
[g] Department of Pharmacology and Molecular Sciences, Johns Hopkins University School of Medicine, Baltimore, MD, 21205, USA
[h] Adrienne Helis Malvin Medical Research Foundation, New Orleans, LA, 70130-2685, USA
[i] Diana Helis Henry Medical Research Foundation, New Orleans, LA, 70130-2685, USA

ARTICLE INFO

Article history:
Received 13 May 2020
Received in revised form 27 October 2020
Accepted 4 November 2020

Keywords:
α-Synuclein
Cell-to-cell transmission
Prion-like
Parkinson's disease
Nanozyme

ABSTRACT

Braak's prion-like theory fundamentally subverts the understanding of Parkinson's disease (PD). Emerging evidence shows that pathologic α-synuclein (α-syn) is a *prion*-like protein that spreads from one region to another in PD brain, which is an essential driver to the pathogenesis of PD. Thus far, there is a big knowledge gap that limited nanomaterial that can block prion-like spreading. Here, α-syn preformed fibrils (PFF) are used to model prion-like spreading and biocompatible antioxidant nanozyme, PtCu nanoalloys (NAs), is applied to fight against α-syn spreading. The results show that PtCu NAs significantly inhibit α-syn pathology, cell death, and neuron-to-neuron transmission by scavenging reactive oxygen species (ROS) in primary neuron cultures. Moreover, the PtCu NAs significantly inhibit α-syn spreading induced by intrastriatal injection of PFF. It is the first time to observe nanozyme can block prion-like spreading, which provides a proof of concept for nanozyme therapy. It is also anticipated that the biomedical application of nanozyme against prion-like spreading could be optimized and considered to be developed as a therapeutic strategy against Parkinson's disease, Alzheimer's disease, and other prion-like proteinopathies.

Introduction

Parkinson's disease (PD) is the second most common neurodegenerative disorder characterized with misfolded α-synuclein (α-syn) accumulation in Lewy bodies (LB) [1,2]. Although some α-syn mutations have been linked to familial PD [3,4], the majority cases are sporadic with unknown etiology [5]. Recently, Braak's theory fundamentally subverts the understanding of PD [5,6] that pathologic α-syn is a *prion*-like protein spreading in PD brain, which drivers the pathogenesis [7,8]. Substantial postmortem evidence further supports the game-changing discovery [9–11] and prion-like spreading is widely found in other neurodegeneration, including Alzheimer's disease (AD) and amyotrophic lateral sclerosis (ALS) [12–17].

Emerging evidence shows that oxidative stress is an unavoidable pathogenesis factor contributing to prion-like spreading [18–20]. For example, paraquat can induce oxidative stress *in vivo* and *in vitro*, which remarkably leads to increased α-syn spreading [20–22]. We have determined that pathologic α-syn can activate

* Corresponding author at: Institute for Cell Engineering, Johns Hopkins University School of Medicine, Baltimore, MD, 21205, USA.
** Corresponding authors.
E-mail addresses: liym@mail.tsinghua.edu.cn (Y.-M. Li), zzheng@xcu.edu.cn (Z. Zheng), heweiweixcu@gmail.com (W. He), xmao4@jhmi.edu (X. Mao).
[1] These authors contributed equally to this work.

https://doi.org/10.1016/j.nantod.2020.101027
1748-0132/

nitric oxide synthase (NOS), resulting in increased NO level and DNA damage *in vitro*, and facilitating α-syn spreading and severe neurodegeneration and behavioral deficits *in vivo* [23]. Of note, the inhibitors of NOS-related pathway can significantly prevent the pathologic α-syn-induced pathogenesis and pathology spreading [23], which indicates that reducing the level of oxidative stress may be an effective way against pathologic α-syn spreading in PD.

Tremendous efforts have been made to develop a sporadic PD model with α-syn spreading model for mechanism study and therapeutic development [23–29]. The α-syn preformed fibrils (PFF) model is groundbreaking that a single injection of recombinant α-syn PFF can replicate LB-like pathology spreading, neurotoxicity and motor/non-motor dysfunction in wildtype mice [7,30,31]. The PFF model can perfectly mimic the sporadic PD; however, limited nanomaterial was reported that can prevent prion-like spreading [32]. Another critical issue is the biological effect of nanomaterial. Metal oxides nanoparticles are prone to cause uncertain biological effects because of unstable multivalent metals on the surface. Noble metal (alloy) nanostructures with stable zero-valent metal surfaces and adjustable catalytic activity can overcome this problem. Since there is a big knowledge gap to identify nanomaterials can block spreading and we have reported that metallic nanoparticles exhibit multiple enzyme-like and efficient antioxidant activity to reduce reactive oxygen species (ROS) production [33,34]. We sought to explore the potential of metal alloy nanozymes in preventing prion-like spreading induced by oxidative stress in the sporadic PD model.

To address the question that nanozyme can prevent prion-like spreading, we proposed a series of *in vitro* and *in vivo* experiments. We generated the PtCu bimetallic nanoalloys (NAs) with strong antioxidant ability, and applied the biocompatible agents in PFF-induced cellular and animal models. The PtCu NAs have a remarkable ability of scavenging ROS in primary neuron cultures induced by the administration of PFF, and subsequently inhibited α-syn pathology, neurotoxicity, and neuron-to-neuron transmission *in vitro*. The PtCu NAs further exhibited significant inhibition on pathologic α-syn spreading in the mouse brain induced by an intrastriatal injection of PFF. To our best knowledge, it is the first time to determine that nanozyme can block pathologic α-syn cell-to-cell transmission, which provides a proof of concept for the efficacy of nanozymes against prion-like spreading in neurodegeneration. It is also anticipated that biomedical application of nanozyme against prion-like spreading could be optimized and considered to be developed as a novel therapeutic strategy against PD, AD, and other prion-like proteinopathies.

Results

Formation and the antioxidant activity of PtCu NAs

The PtCu NAs were prepared by hydrothermal reduction of $PtCl_4^{2-}$ and Cu^{2+} in the presence of polyvinyl pyrrolidone (PVP) and glycine. The PtCu NAs are well dispersed and uniform spherical shaped, also shows the detail with scraggy surfaces (Fig. 1

a). The zeta-potential of PVP coated PtCu NAs was determined to be -15.3 ± 1.5 mV. The PtCu NAs suspension shows a good stability against aggregation during long-term storage. The high-resolution TEM (HRTEM) further indicates the well-defined lattice planes in part of single particles (Fig. S1a). The calculated lattice spacing is 0.218 nm, which corresponds to the distance of (111) facet and falls between the values for Pt (0.228 nm) and Cu (0.208 nm). The X-ray photoelectron spectroscopy (XPS) survey spectra and energy-dispersive X-ray spectroscopy (EDS) analysis confirmed the co-existence of element Pt and Cu (Figs. 1b, S2), and the measured Pt/Cu molar ratio of 1.2 is consistent with the seeded Pt^{2+}/Cu^{2+} ratio. The average diameter of the PtCu NAs was calculated to be 32.1 ± 4.5 nm (Fig. S1c). The diffraction peaks of X-ray diffraction (XRD) indexed to the planes (111) and (200) and was, as expected, located between the corresponding peaks of pure Pt and Cu (Fig. 1c). These confirmed the formation of bimetallic alloy and the lattice parameter varying along with the alloy composition.

The antioxidant capability of the PtCu NAs was reflected in their catalytic activity toward hydrogen peroxide reduction (peroxidase-like and catalase-like), superoxide disproportionation reaction (superoxide dismutase (SOD)-like) and clearance of free radicals. The PtCu NAs can accelerate the consumption of H_2O_2 in two ways: (I) catalyzing the H_2O_2 reduction *via* peroxidase-like activity and (II) catalyzing the H_2O_2 decomposition *via* catalase-like activity (Fig. 1d). Firstly, the peroxidase-like activity of PtCu NAs was compared with horseradish peroxidase (HRP). We find that PtCu NAs, behaving like HRP, can quickly catalyze the redox reaction between H_2O_2 and 3,3′,5,5′-tetramethylbenzidine (TMB) and lead to a reduction of H_2O_2 and oxidation of TMB, which generates characteristic absorption peaks at 450 nm and 650 nm (Figs. S3a, 1 e). The PtCu NAs and HRP show the same trend on the dosage-dependent activity, 4.12 μg/mL PtCu NAs is equivalent to 1 U/mL HRP to accelerate the oxidation of TMB by H_2O_2 (Figs. S3b, 1 f).

Catalase is an intracellular enzyme present in most aerobic cells. Its function to catalyze the decomposition of H_2O_2, makes it potentially useful in protection against oxidative stress. To investigate the catalase-like activity of PtCu NAs, we employed both UV–vis spectra and electron spin resonance (ESR) oximetry to monitor the reduction of H_2O_2 and production of O_2, respectively. Compared to control, the addition of PtCu NAs resulted in a significant decrease of H_2O_2 absorbance as a function of time, suggestive of that the PtCu NAs behave like catalase in the decomposition of H_2O_2 (Fig. S4a). To further determine if molecular oxygen was generated, we conducted ESR oximetry in conjunction with spin-label 4-oxo-2,2,6,6-tetramethyl piperidine-d_{16}-1-^{15}N-oxyl (PDT). ESR oximetry is based on the physical collision between molecules oxygen (O_2) and spin labels (PDT was used here). Because O_2 is paramagnetic, the collision between the PDT molecules and O_2 produces spin exchange, which leads to a shorter relaxation time and consequently causing the ESR spectrum of PDT a broader line width and lower peak intensity. The degree of spin exchange is dependent on the concentration of O_2, a subtle change of O_2 results in a corresponding response in the line width of ESR spectrum [35]. When mixed the PtCu NAs and H_2O_2, a time-dependent increase in line width and a decrease in peak intensity of the ESR signal indicates the dioxygen production (Fig. 1g). Furthermore, it was found that the decomposition rate of H_2O_2 was strongly dependent on the concentration of PtCu NAs. With increasing the concentration of PtCu NAs from 2.16–21.58 μg/mL, we observed a gradual acceleration of the decomposition of H_2O_2 (Fig. S4b).

As a specific enzyme for degrading superoxide, SOD plays a critical role in ROS balance and acts as an antioxidant to protect cellular components against oxidative damage by superoxide. To verify SOD-like activity, superoxide was generated *in situ* by the classic KO_2 system in the presence of crown ether in an aprotic solvent. The capability of PtCu NAs to scavenge superoxide was firstly verified by a nitroblue tetrazolium (NBT) assay (Figs. S5a, S5b). The SOD-like activity was further verified by ESR technique, in which 5-tert-butoxycarbonyl 5-methyl-1-pyrroline N-oxide (BMPO) is used as a typical spin trap for superoxide. Adding KO_2 to the solution containing BMPO produced a strong ESR signal attributable to BMPO/•OOH (Fig. 1h). As expected, the ESR signal intensity decreased greatly when SOD or PtCu NAs was added, suggesting again their catalytic ability to scavenge O_2^{-}•. The scavenging efficiency of 10 μg/mL PtCu NAs was comparable with that of 5 U/mL natural SOD, suggestive of the excellent SOD-like activity of PtCu NAs. In addition, the antioxidant capability of PtCu NAs was also reflected in their abil-

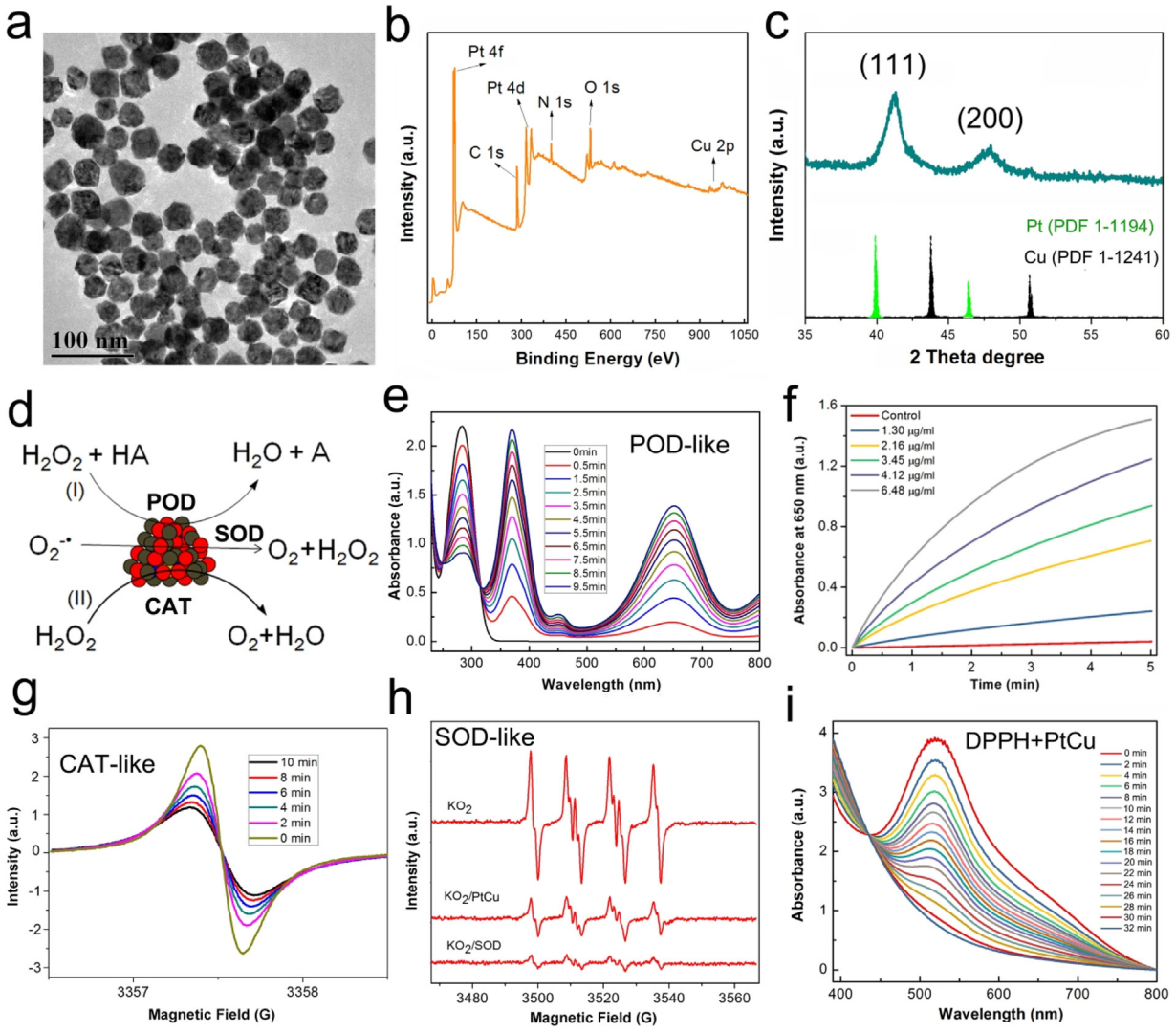

Fig. 1. Formation of PtCu NAs and antioxidant capability *via* peroxidase, catalase, SOD-like activities and scavenging free radicals. **a** Transmission electron microscopy (TEM), **b** XPS survey and **c** X-ray diffraction (XRD) pattern of PtCu NAs with Pt/Cu molar ratio of 1/1. **d** the scheme for PtCu NAs to mimic 3 redox enzymes (POD: peroxidase, SOD: superoxide dismutase, CAT: catalase). **e** The UV–vis spectra of TMB in the presence of H_2O_2 catalyzed by POD-like PtCu NAs. **f** the absorbance in the function of time under different dosage of PtCu NPs. **g** The CAT-like activity of PtCu NPs to reduce H_2O_2 demonstrated by electron spin resonance (ESR) oximetry, the evolution of ESR spectra of PDT over time in the presence of 2 mM H_2O_2 before and after addition of PtCu NPs in a closed chamber. **h** the SOD-like activity of PtCu NAs to reduce superoxide demonstrated by ESR spectroscopy. **i** DPPH radicals scavenging activity of PtCu NPs in time dependent manner.

ity to reduce free radicals. 2,2-diphenyl-1-picrylhydrazyl (DPPH), a well-known stable radical that widely used for the quantitative determination of antioxidant capacity, was selected for evaluating the antioxidant activity of PtCu NAs. DPPH itself is stable to be reduced without the help of catalysts over the testing time (Fig. S6). We found that each PtCu NAs and antioxidant can efficiently scavenge the DPPH radical in a time- and concentration-dependent manner, demonstrating their antioxidant capability (Figs. 1i, S7). Ascorbic acid (AA) shows the fast antioxidant effect and its antioxidant capability is dependent on the concentration (Fig. S7). We find that the antioxidant mechanism between PtCu NAs and AA is quite different. AA playing an antioxidant effect is through its own chemical oxidation as sacrificing, while the antioxidant effect of PtCu NAs was from its catalytic nature to facilitate electrons' transfer. Therefore, PtCu NAs can be recycled to reduce DPPH until DPPH is consumed, but AA needs to be added by a considerable concentration to consume DPPH.

To study the effect of alloy composition on enzyme-like activities, we have prepared PtCu nanoalloys with Pt/Cu atomic ratio of 1/3 and 3/1, respectively. By simply changing the molar ratio of added Pt^{2+}/Cu^{2+}, the PtCu NAs with tunable chemical composition were prepared. TEM images displayed that PtCu NAs prepared under each of Pt^{2+}/Cu^{2+} ratio showed the well dispersed and uniform shape (Fig. S8). The particle size decreased gradually when changing the PtCu ratio from 3/1 (41.5 ± 5.7) to 1/3 (22.2 ± 2.4 nm) (Fig. S8d). Fig. S9 summarizes the dependence of measured Pt content, particle size and D value of (111) plane on the calculated Pt content. The measured Pt content linearly increased with the increasing addition of Pt^{2+}. The linear relationship has a slope near 1.0 which indicates a complete reduction of Cu^{2+} and Pt^{2+} to form the PtCu alloy NPs. All these characterizations demonstrated that, by changing the added amount of Pt^{2+}/Cu^{2+}, fine tuning of particle size, alloy composition and crystal structure of PtCu NAs are achieved. For better comparison, the monometallic Pt and Cu NPs were also prepared using the same procedure to PtCu NAs. The multiple enzyme-like (peroxidase-like, catalase-like and SOD-like) activities of different PtCu NAs, Pt and Cu NPs were investigated (Fig. S10). It was found that the enzyme-like activity of PtCu NAs was strongly dependent on their chemical compositions, and alloying with Cu at the percentage of ~25 % can evidently increase the

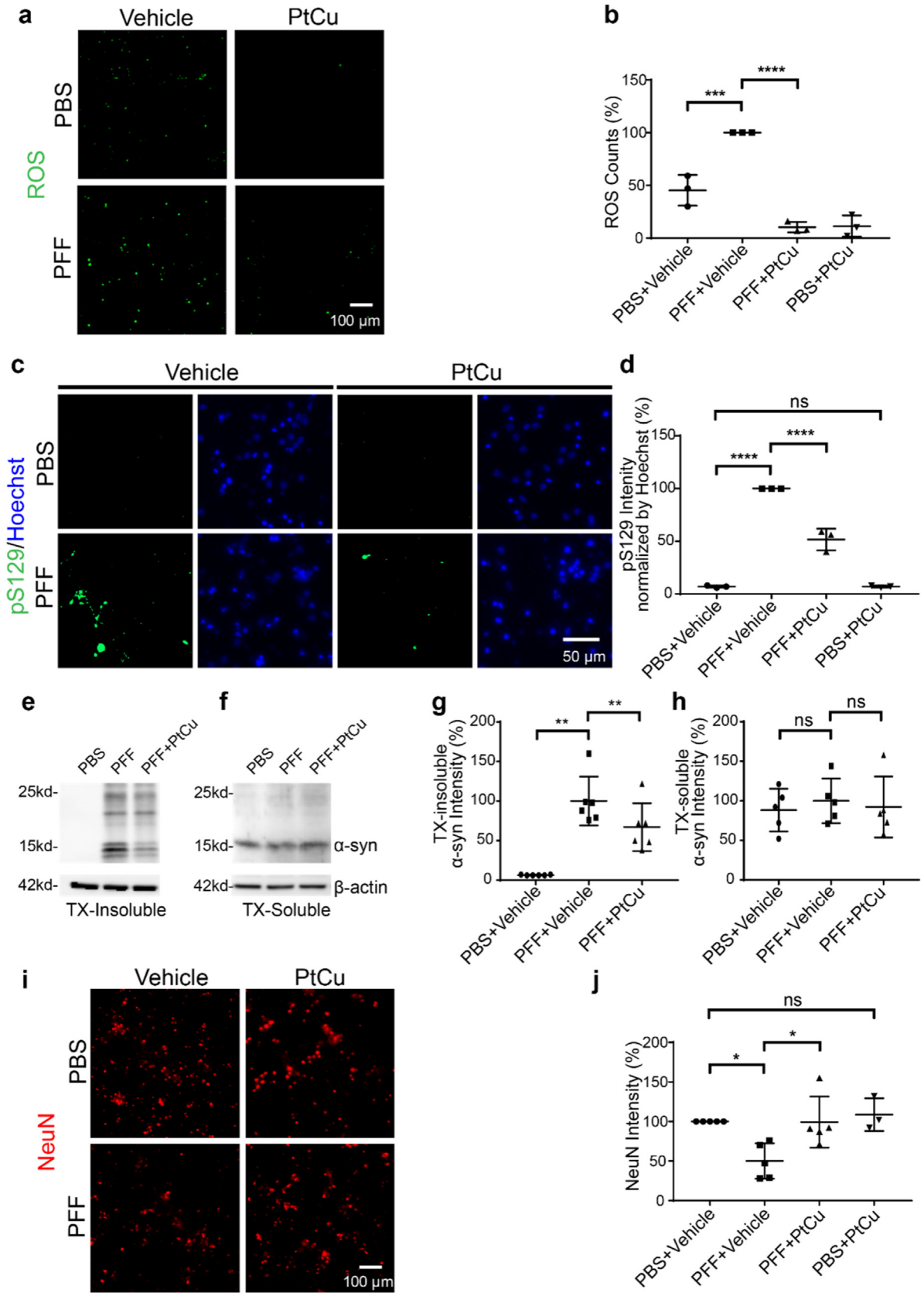

Fig. 2. PtCu NAs reduce the reactive oxygen species (ROS), α-syn pathology and neurotoxicity induced by PFF *in vitro*. **a** PtCu NAs reduce the ROS induced by PFF. PFF (10 μg/mL) and PtCu NAs (1 μM) were added into mouse primary neurons seven days *in vitro*. To assess the ROS level, the neurons were incubated with CM-H2DCFDA (2 μM) for 30 min, two days after PFF treatment. Scale bar, 100 μm. **b** Quantification of the ROS level. Data are the means ± SD, $n = 3$ independent experiments, one-way ANOVA followed by Tukey's correction. **c** PtCu NAs reduce the pS129 immunoreactivity induced by PFF. Neurons seven days *in vitro* were treated with PFF and PtCu/Vehicle, the level of pS129 immunoreactivity was assessed with anti-pS129 at seven days after treatment. Scale bar, 50 μm. **d** Quantification of the pS129 immunoreactivity. Data are

enzyme-like activity of Pt NPs. The same trends were observed for peroxidase-like, catalase-like and SOD-like activity, with increasing the Pt content in PtCu bimetallic alloy, the activity gradually increased.

PtCu NAs decrease the level of ROS in primary cortical neurons induced by α-syn PFF

To determine the clearance effect of PtCu NAs on cellular ROS induced by PFF, purified α-syn monomer were agitated for mature fibrils (~7 days) and then sonicated into PFF following the established protocol [29]. The TEM images indicate that PFF is short fibrils (~45 nm) and α-syn monomer has no regular structures (Figs. S11a, S11b), which is consistent with the previous publication [29]. The immunoblot of PFF further validates the α-syn aggregation, compared to the α-syn monomer (Fig. S11c). We used a thioflavin T assay and determined that PFF exhibits increased ThT fluorescent intensity compared to the α-syn monomer (Fig. S11d). To determine if PtCu NAs can directly modulate α-syn aggregation, we have performed the fibrillization experiments. The results show that no appreciable modulation on α-syn aggregation can be observed in the presence of PtCu NAs in the Thioflavin T (ThT) assay (Fig. S12a) and the immunoblot (Fig. S12b). These results indicate that PtCu NAs do not directly affect the aggregation of α-syn.

Exogenous PFF was administered into mouse primary neurons seven days *in vitro* (10 μg/mL) and incubated for two days. We assessed the level of ROS by CM-H2DCFDA kit (Thermo Fisher Scientific, Waltham, MA, USA), and determined that the level of ROS significantly increased in neurons two days after PFF administration, compared to PBS-treated neurons (Fig. 2a,b). In contrast, PtCu NAs significantly decreased the level of ROS in neurons treated with PFF (Fig. 2a,b). In brief, the results show that PFF significantly induced the increased level of ROS in primary neurons, and PtCu NAs significantly decreased the ROS production induced by PFF, which is consistent with that in the cell-free system.

PtCu NAs decrease the α-syn pathology in primary cortical neurons induced by α-syn PFF

We then asked whether PtCu NAs can decrease the α-syn pathology in neurons induced by PFF. Exogenous PFF was treated into primary neurons seven days *in vitro* (10 μg/mL) and the α-syn pathology was assessed seven days post administration, including the phosphorylated serine129 α-syn (pS129) and insoluble α-syn aggregates. pS129 is a typical pathological marker in PD, which has been widely applied for assessing the levels of α-syn pathology and transmission [7,23,29,36]. As published previously [29], PFF induced a substantial amount of pS129 immunoreactivity in neurons, compared to PBS-treated neurons (Fig. 2c,d). Treatment with PtCu significantly decreased the amount of pS129 immunoreactivity in PFF-treated neurons (~50 % less) (Fig. 2c,d).

PFF and PtCu NAs were administered to primary neurons, we examined α-syn level from lysates sequentially extracted in 1% Triton X-100 (soluble fraction) and 2% SDS (insoluble fraction) seven days after administration. Substantial insoluble α-syn was observed (Fig. 2e,g) in PFF-treated neurons, whereas PtCu NAs significantly decreased the amount of insoluble α-syn induced by PFF (Fig. 2e,g). There is no significant difference in the amount of soluble α-syn between PFF and PFF + PtCu group (Fig. 2f,h). These data show that the administration of PFF significantly induced the α-syn pathology *in vitro*, and treatment with PtCu significantly reduced the α-syn pathology, including the pS129 and insoluble α-syn.

PtCu NAs inhibit the α-syn PFF-induced neurotoxicity in primary cortical neurons

Not only the α-syn pathology, PFF can further induce substantial neurotoxicity. To determine the inhibitory efficacy of PtCu NAs in PFF-induced neurotoxicity, we administered PFF (10 μg/mL) into primary neurons seven days *in vitro* and assessed neurotoxicity with anti-NeuN (neuronal nuclei) immunoreactivity 15 days afterward. PFF induced substantial neurotoxicity as previously described [29], compared to PBS-treated neurons (Fig. 2i,j). In contrast, PtCu NAs significantly inhibited neurotoxicity in PFF-treated neurons (~ 50 % less) (Fig. 2i,j). It is noted that there is no significant difference in the neurotoxicity between vehicle- and PtCu-treated neurons (Fig. 2i,j). The brightfield images showed the similar results (Figs. S13a, S13b). These data show that PtCu NAs significantly inhibited the neurotoxicity induced by PFF, and PtCu NAs alone did not exhibit any appreciable neurotoxicity.

PtCu NAs block the α-syn cell-to-cell transmission induced by PFF in vitro.

A microfluidic neuronal culture device with two chambers connected in tandem by a series of microgrooves (eNUVIO, Quebec, Canada) was used to determine the efficacy of PtCu NAs in blocking α-syn transmission *in vitro* (Fig. 3a) [23,29]. As indicated, both chamber 1 and chamber 2 were planted with primary neurons, and the medium volume in chamber 1 is 40 μL lower than the one in chamber 2 in order to prevent diffusion of PFF (from chamber 1) to chamber 2 (Fig. 3a). PFF was administered into the neurons seven days *in vitro* in chamber 1, and PtCu NAs or vehicle control were simultaneously treated into the neurons in chamber 2 (Fig. 3a). Transmission of pathologic α-syn was monitored by pS129 immunoreactivity seven days after PFF was administered, as previously described [29]. Administration of PFF led to a substantial amount of pS129 immunoreactivity in chamber 1 (Fig. 3b), and there is no significant difference in the pS129 intensity in chamber 1 between the PFF-vehicle group and the PFF-PtCu group (Fig. 3c), which indicates the original pathologic α-syn source is at the same level for spreading. To assess the transmission of pathologic α-syn along dendrites and axons, we further examined the levels of pS129 in chamber 2. Substantial pS129 immunoreactivity was observed in vehicle-treated neurons in chamber 2 (Fig. 3b), whereas a significant reduction of the amount of pS129 immunoreactivity was assessed in PtCu-treated neurons in chamber 2 (Fig. 3c). Of note, α-syn aggregation is one step of pathologic α-syn cell-to-cell transmission and we have determined that PtCu NAs cannot mediate α-syn aggregation in the fibrillization assay (Fig. S12). Taken together, these data indicate the inhibitory efficacy of PtCu NAs in pathologic α-syn cell-to-cell transmission induced by PFF.

the means ± SD, n = 3 independent experiments, one-way ANOVA followed by Tukey's correction. **e, f** Immunoblots of α-syn in the soluble and insoluble fractions. Neurons at seven days *in vitro* were treated with PFF and PtCu/Vehicle. Seven days after treatment, neuron lysates were extracted with 1% TX-100 for TX-soluble fraction followed by 2% SDS for TX-insoluble fraction. α-Syn level was assessed by anti-α-syn antibody. **g, h** Quantification of the insoluble (left panel) and soluble (right panel) α-syn. Data are the means ± SD, n = 5-6 independent experiments, one-way ANOVA followed by Tukey's correction. **i** PtCu NAs block the neurotoxicity induced by PFF. The toxicity assay was performed 15 days after PFF treatment, which was assessed by anti-NeuN immunostaining. Scale bar, 100 μm. *j* Quantification of the neurotoxicity. Data are the means ± SD, n = 3-5 independent experiments, one-way ANOVA followed by Tukey's correction. $^{*}P < 0.05$, $^{**}P < 0.01$, $^{***}P < 0.001$, $^{****}P < 0.0001$, ns, non-significant.

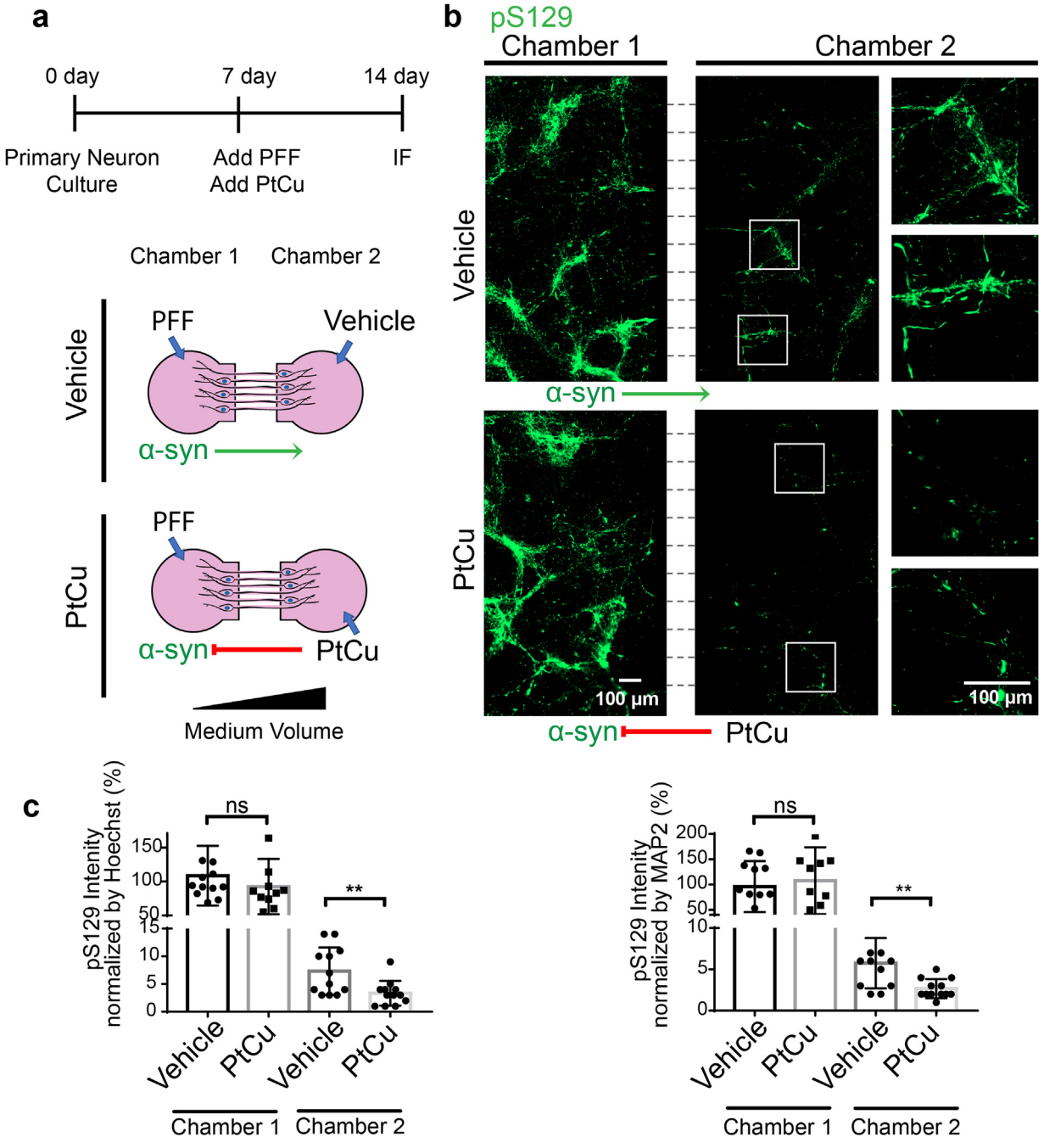

Fig. 3. PtCu NAs inhibit α-syn transmission *in vitro*. **a** Timeline of α-syn transmission *in vitro* experiment (top) and the experimental design with PtCu NAs treatment in microfluidic chamber (bottom). Neurons were cultured in chamber 1 and chamber 2. PFF were added to neuron cultures at 7 days *in vitro* in chamber 1. PtCu NAs (1 μM) was treated simultaneously into neuron cultures in chamber 2. Neurons were fixed with 4% PFA seven days after treatment for immunostaining. **b** pS129 Immunostaining for α-syn transmission. Neurons were immunostained with anti-pS129 antibody. Scale bar, 100 μm. **c** Quantification of pS129 immunostaining. Data are the means ± SD, $n = 4$ independent experiments, unpaired Student's *t*-test. $^{**}P < 0.01$, ns, non-significant.

The inhibitory effect of PtCu in α-syn spreading induced by α-syn PFF in vivo

To determine the effect of PtCu in inhibiting α-syn spreading *in vivo*, we stereotactically injected PFF into the dorsal striatum of wild-type mice at two-months old, and treated PtCu into the substantia nigra (SN) simultaneously (Fig. 4a). Intrastriatal injection of PFF can spread from the striatum to the substantia nigra in months [29], and it is expected that the treatment with PtCu in the SN can prevent α-syn transmission. The mice were sacrificed two months after PFF injection (Fig. 4a). By assessing the pS129 immunoreactivity, we found that a substantial amount of pS129 immunoreactivity in the SN of PFF-injected mice treated with vehicle (Fig. 4b,c) as previously published [29]. In contrast, PtCu NAs significantly reduced the amount of pS129 immunoreactivity in the SN of PFF-injected mice (Fig. 4b,c). There is no significant difference in the pS129 levels in the striatum of PFF-injected mice between PtCu and vehicle treatment (Fig. 4b,d), indicating the successful stereotaxic injection surgery of PFF.

To assess the pathologic α-syn spreading *in vivo*, the SN and striatum regions were collected from PFF-injected mice with treatment with PtCu or vehicle. We obtained the insoluble and soluble

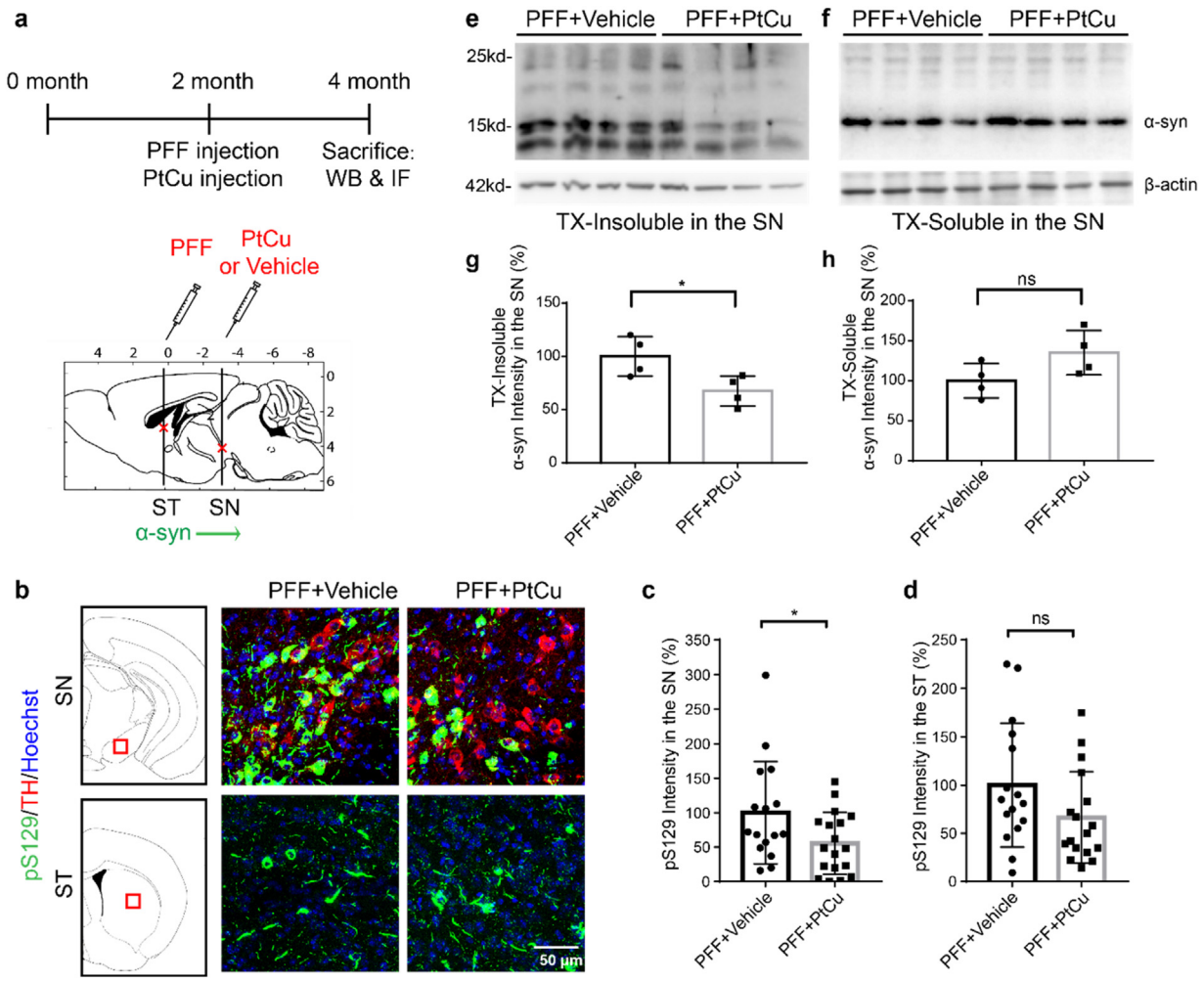

Fig. 4. PtCu NAs inhibit α-syn transmission *in vivo*. **a** Timeline of PFF animal experiments with PtCu NAs treatment (top) and the stereotaxic injection sites of PFF and PtCu/Vehicle (bottom). Mice were stereotaxically injected with PFF and PtCu/Vehicle at 2-months old, and were sacrificed at two months after PFF injection. **b** pS129 immunostaining in the substantia nigra (SN) and striatum (ST). Brain sections were stained with anti-pS129 antibody and anti-TH (Tyrosine Hydroxylase) antibody. Scale bar, 50 μm. **c, d** Quantification of pS129 immunostaining. Data are the means ± SD, $n = 6$ mice per group, unpaired Student's t-test. $^*P < 0.05$, ns, non-significant. **e, f** Immunoblots of brain lysates of the SN. Brain lysates were extracted with 1% TX-100 for TX-soluble fraction followed by 2% SDS for TX-insoluble fraction. Total α-syn level was evaluated by anti-α-syn antibody. **g, h** Quantification of immunoblots of brain lysates. Data are the means ± SD, $n = 4$ mice per group, unpaired Student's t test. $^*P < 0.05$, ns, non-significant.

fractions from the brain lysates and assessed the expression levels of insoluble and soluble α-syn by immunoblots. Substantial insoluble α-syn was observed in the SN region of PFF-injected mice with vehicle treatment (Fig. 4e,g), whereas PtCu NAs significantly reduced the amount of insoluble α-syn (Fig. 4e,g). There is no significant difference in the amount of insoluble α-syn in the striatum of PFF-injected mice between PtCu and vehicle treatment (Fig. S14a, S14c), further indicating the accurate injection location of PFF. The amount of soluble α-syn in the SN and striatum was also examined, exhibiting no significant difference (Figs. 4f,h, S14b, S14d). These data taken together show that treatment with PtCu NAs significantly reduced α-syn transmission induced by PFF *in vivo*.

Discussion

The major discovery of our present paper is that the noble bimetallic nanozyme is capable of blocking pathologic α-syn cell-to-cell transmission by scavenging the ROS induced by PFF. We synthesized the PtCu NAs, and determined that PtCu has the remarkable antioxidant ability in cell-free systems, reduced cellular ROS, α-syn pathology, neurotoxicity, and transmission in a sporadic PD cellular model by using PFF. Moreover, treatment with PtCu significantly blocked α-syn spreading from the striatum to the substantia nigra *in vivo* (Fig. 5).

It is the first time to determine nanozyme can block α-syn spreading. Prior studies have reported that nanozymes CeO_2, Mn_3O_4, and Cu_xO mimicking antioxidant enzymes reducing reactive oxygen species (ROS) production can prevent neurodegeneration in neurotoxin (MPTP)-induced PD model [37–40]. However, MPTP model lacks α-syn pathology that is not a sporadic PD model [41,42]. Thus, the present study fills up the disconnection with clinical observation for α-syn pathology significantly impedes the evaluation of the efficacy of nanomaterials in PD. It is also noted that our work focused on the prevention on pathologic α-syn transmission 2-month after PFF injection. Since intrastriatal injection of α-syn PFF can induce motor dysfunction 6-months after injection [23,29]. We will determine if PtCu NAs can mediate the neurodegeneration (*e.g.* behavioral deficits) induced by α-syn PFF in the future studies.

Considering the diverse biological microenvironments may affect the performance of the PtCu NAs, we have assessed the antioxidant ability of the PtCu NAs at pH = 4.5, 5.5, 6.5 and 7.5 [43]. The results verify that pH could affect the antioxidant activity of the PtCu NAs, and relatively high pH facilitates the antioxidant capability (Figs. S15–S17). Furthermore, we determined that the

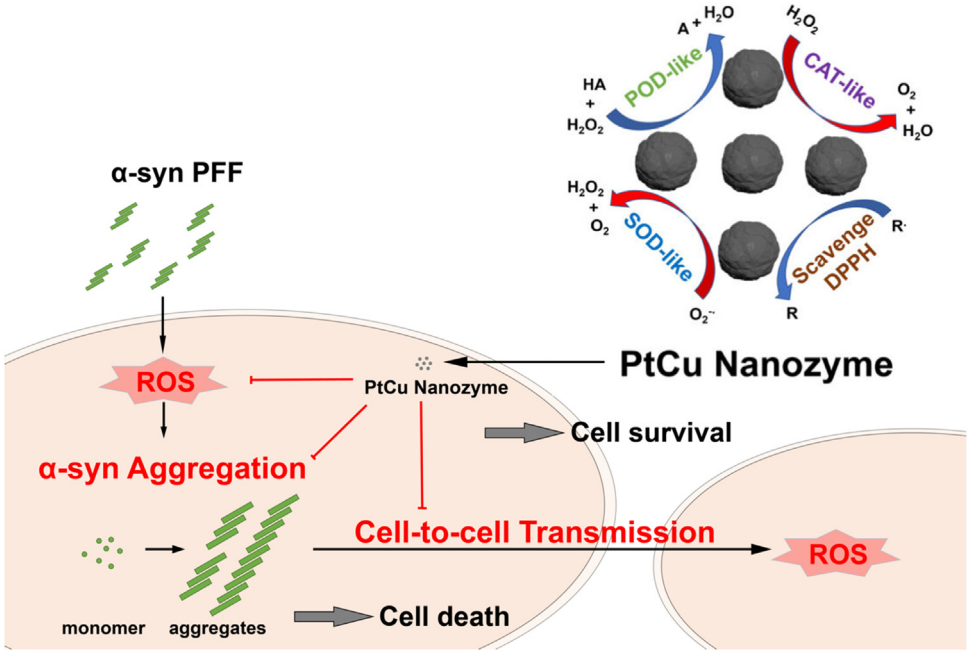

Fig. 5. Schematic summary for the PtCu nanozyme scavenging ROS and preventing pathologic α-Synuclein-induced pathology, neurotoxicity and cell-to-cell transmission *in vitro* and *in vivo*. Synthetic PtCu NAs functionally mimic three redox enzymes, including peroxidase (POD), catalase (CAT) and superoxide dismutase (SOD), scavenge free radicals (DPPH), and show superior antioxidant capability in a cell-free system. In sporadic PD models, administration of PFF in neuron culture induces increased ROS, α-syn aggregation, pathology and neurotoxicity. Furthermore, PFF-induced aggregates can further cause cell-to-cell transmission and neurodegeneration. The PtCu NAs act as nanozyme that scavenges ROS, and significantly reduce PFF-induced pathology, neurotoxicity, and cell-to-cell transmission.

formation of protein-corona could reduce the antioxidant activity of the PtCu NAs (Fig. S18). Consistent with the published reports [44,45], biological microenvironment may affect the enzyme-like activity of the PtCu NAs. Importantly, our *in vitro* and *in vivo* results have shown that the PtCu NAs can significantly reduce the ROS production induced by PFF and subsequent α-syn pathology spreading.

Compared to metal oxides, metal and metal-based nanozymes have advantages such as defined and controllable structures, easy surface modification, good biocompatibility, and tunable enzyme-like activity to scavenge ROS. Metal-based nanozymes may also be applied to neural regeneration application, treatment of brain injury and cerebral malaria due to resent publications [46–49]. Especially, when downsizing the particle to sub-nanometer or even single state atoms, the metal-based nanozymes will exhibit significantly increased catalytic activity [50,51]. Benefitting from the advances in catalytic chemistry, therefore, metal-based (especially single atom) nanozymes are expected to show a great promise in PD treatment. However, there are many unknowns about metal NPs in the central nervous system that may hinder the efficacy including the biosafety, the blood-**brain** barrier (BBB) permeability, the acute and long-term effect, *etc*, which inspired us to explore in the future.

PtCu NAs exhibit peroxidase, catalase, and SOD-like activity as well as the ability to scavenge free radicals (DPPH), which make PtCu NAs an excellent antioxidant that reduces ROS production. Graphene quantum dots have been applied to prevent α-syn-induced cell-to-cell transmission, by directly interacting with mature fibrils and triggering their disaggregation [32], whereas our present work provides a novel therapeutic strategy to prevent cell-to-cell transmission of α-syn pathology by using nanozyme for clearance of ROS. The therapeutic strategy can also be applied to other neurodegenerative disorders.

We have determined that poly(adenosine 5′-diphosphate–ribose) (PAR) polymerase-1 (PARP-1) was activated in PFF-treated neurons, which results in accumulation of PAR polymer [23]. Importantly, PAR polymer further induced α-syn to form a misfolded compact strain, exhibiting enhanced neurotoxicity [23]. Further studies should be directed to determine the role of PtCu in alleviating the pathogenic generation of NO in neurodegenerative diseases such as PD.

Conclusions

In summary, the PtCu nanozyme exhibits significant efficacy in preventing α-syn prion-like spreading in sporadic PD models. These data taken together provide a concept of proof that the redox nanozyme can be considered to be developed as a therapeutic strategy against pathologic α-syn spreading in PD and related α-synucleinopathies.

Author contributions

Y.Q.L., Y.M.L., W.W.H., X.B.M. conceived and designed the experiments; Y.Q.L., X.E.Q. conducted the biochemical, cellular and animal studies and statistical analysis; Y.Y.M., H.M.J., conducted the nanoparticle synthesis and characterization; Y.Q.L., Y.Y.M., E.Q.X., H.M.J., Y.M.L., Z.Z., W.W.H., X.B.M. participated in final data analysis and interpretation; V.L.D., T.M.D., Y.Q.L., Z.Z., W.W.H., X.B.M. wrote and edited the manuscript.

Declaration of Competing Interest

The authors report no declarations of interest.

Acknowledgements

We appreciate Rong Chen from Johns Hopkins University School of Medicine for α-syn preparation. We thank Dr. Yu Chong from Soochow University and Prof. Yongwei Huang from Henan University for their assistance in the additional experiment. This work is supported financially by the National Natural Science Foundation

of China (51772256), the Program for Innovative Research Team (in Science and Technology) in University of Henan Province (19IRTSTHN026), the Program for Zhongyuan Leading Talents of Science and Technology Innovation in Henan Province (204200510016), and National Key R & D Program of China (2018YFA0507600). This work is also supported by grants from Parkinson's Foundation (PF-JFA-1933), Maryland Stem Cell Research Foundation Discovery Award (2019-MSCRFD-4292), American Parkinson's Disease Association and the JPB Foundation. The authors acknowledge the joint participation by the Adrienne Helis Malvin Medical Research Foundation and the Diana Helis Henry Medical Research Foundation through their direct engagement in the continuous active conduct of medical research in conjunction with The Johns Hopkins Hospital and the Johns Hopkins University School of Medicine and the Foundation's Parkinson's Disease Programs H-2018, M-2016, M-2019. T.M.D. is the Leonard and Madlyn Abramson Professor in Neurodegenerative Diseases.

Appendix A. Supplementary data

Supplementary material related to this article can be found, in the online version, at doi:https://doi.org/10.1016/j.nantod.2020.101027.

References

[1] M.G. Spillantini, M.L. Schmidt, V.M. Lee, J.Q. Trojanowski, R. Jakes, M. Goedert, Nature 388 (1997) 839–840, http://dx.doi.org/10.1038/42166.
[2] M. Baba, S. Nakajo, P.H. Tu, T. Tomita, K. Nakaya, V.M. Lee, J.Q. Trojanowski, T. Iwatsubo, Am. J. Pathol. 152 (1998) 879–884.
[3] M.H. Polymeropoulos, C. Lavedan, E. Leroy, S.E. Ide, A. Dehejia, A. Dutra, B. Pike, H. Root, J. Rubenstein, R. Boyer, E.S. Stenroos, S. Chandrasekharappa, A. Athanassiadou, T. Papapetropoulos, W.G. Johnson, A.M. Lazzarini, R.C. Duvoisin, G. Di Iorio, L.I. Golbe, R.L. Nussbaum, Science 276 (1997) 2045–2047, http://dx.doi.org/10.1126/science.276.5321.2045.
[4] J. Simon-Sanchez, C. Schulte, J.M. Bras, M. Sharma, J.R. Gibbs, D. Berg, C. Paisan-Ruiz, P. Lichtner, S.W. Scholz, D.G. Hernandez, R. Kruger, M. Federoff, C. Klein, A. Goate, J. Perlmutter, M. Bonin, M.A. Nalls, T. Illig, C. Gieger, H. Houlden, M. Steffens, M.S. Okun, B.A. Racette, M.R. Cookson, K.D. Foote, H.H. Fernandez, B.J. Traynor, S. Schreiber, S. Arepalli, R. Zonozi, K. Gwinn, M. van der Brug, G. Lopez, S.J. Chanock, A. Schatzkin, Y. Park, A. Hollenbeck, J. Gao, X. Huang, N.W. Wood, D. Lorenz, G. Deuschl, H. Chen, O. Riess, J.A. Hardy, A.B. Singleton, T. Gasser, Nat. Genet. 41 (2009) 1308–1312, http://dx.doi.org/10.1038/ng.487.
[5] H. Braak, K. Del Tredici, U. Rub, R.A. de Vos, E.N. Jansen Steur, E. Braak, Neurobiol. Aging 24 (2003) 197–211.
[6] H. Braak, E. Braak, J. Neurol. 247 (Suppl. 2) (2000) II3–10, http://dx.doi.org/10.1007/PL00007758.
[7] K.C. Luk, V. Kehm, J. Carroll, B. Zhang, P. O'Brien, J.Q. Trojanowski, V.M. Lee, Science 338 (2012) 949–953, http://dx.doi.org/10.1126/science.1227157.
[8] S.B. Prusiner, A.L. Woerman, D.A. Mordes, J.C. Watts, R. Rampersaud, D.B. Berry, S. Patel, A. Oehler, J.K. Lowe, S.N. Kravitz, D.H. Geschwind, D.V. Glidden, G.M. Halliday, L.T. Middleton, S.M. Gentleman, L.T. Grinberg, K. Giles, Proc. Natl. Acad. Sci. U. S. A. 112 (2015) E5308–5317, http://dx.doi.org/10.1073/pnas.1514475112.
[9] J.Y. Li, E. Englund, J.L. Holton, D. Soulet, P. Hagell, A.J. Lees, T. Lashley, N.P. Quinn, S. Rehncrona, A. Bjorklund, H. Widner, T. Revesz, O. Lindvall, P. Brundin, Nat. Med. 14 (2008) 501–503, http://dx.doi.org/10.1038/nm1746.
[10] J.H. Kordower, Y. Chu, R.A. Hauser, T.B. Freeman, C.W. Olanow, Nat. Med. 14 (2008) 504–506, http://dx.doi.org/10.1038/nm1747.
[11] W. Li, E. Englund, H. Widner, B. Mattsson, D. van Westen, J. Latt, S. Rehncrona, P. Brundin, A. Bjorklund, O. Lindvall, J.Y. Li, Proc. Natl. Acad. Sci. U. S. A. 113 (2016) 6544–6549, http://dx.doi.org/10.1073/pnas.1605245113.
[12] J.L. Guo, V.M. Lee, Nat. Med. 20 (2014) 130–138, http://dx.doi.org/10.1038/nm.3457.
[13] P. Brundin, R. Melki, R. Kopito, Nat. Rev. Mol. Cell Biol. 11 (2010) 301–307, http://dx.doi.org/10.1038/nrm2873.
[14] A. Aguzzi, L. Rajendran, Neuron 64 (2009) 783–790, http://dx.doi.org/10.1016/j.neuron.2009.12.016.
[15] F. Clavaguera, T. Bolmont, R.A. Crowther, D. Abramowski, S. Frank, A. Probst, G. Fraser, A.K. Stalder, M. Beibel, M. Staufenbiel, M. Jucker, M. Goedert, M. Tolnay, Nat. Cell Biol. 11 (2009) 909–913, http://dx.doi.org/10.1038/ncb1901.
[16] S. Porta, Y. Xu, C.R. Restrepo, L.K. Kwong, B. Zhang, H.J. Brown, E.B. Lee, J.Q. Trojanowski, V.M. Lee, Nat. Commun. 9 (2018) 4220, http://dx.doi.org/10.1038/s41467-018-06548-9.
[17] M.S. Feiler, B. Strobel, A. Freischmidt, A.M. Helferich, J. Kappel, B.M. Brewer, D. Li, D.R. Thal, P. Walther, A.C. Ludolph, K.M. Danzer, J.H. Weishaupt, J. Cell Biol. 211 (2015) 897–911, http://dx.doi.org/10.1083/jcb.201504057.
[18] E. Paxinou, Q. Chen, M. Weisse, B.I. Giasson, E.H. Norris, S.M. Rueter, J.Q. Trojanowski, V.M. Lee, H. Ischiropoulos, J. Neurosci. 21 (2001) 8053–8061.
[19] O. Scudamore, T. Ciossek, J. Neuropathol. Exp. Neurol. 77 (2018) 443–453, http://dx.doi.org/10.1093/jnen/nly024.
[20] R.E. Musgrove, M. Helwig, E.J. Bae, H. Aboutalebi, S.J. Lee, A. Ulusoy, D.A. Di Monte, J. Clin. Invest. 130 (2019) 3738–3753, http://dx.doi.org/10.1172/JCI127330.
[21] K.C. Luk, J. Clin. Invest. 129 (2019) 3530–3531, http://dx.doi.org/10.1172/JCI130351.
[22] A.L. McCormack, M. Thiruchelvam, A.B. Manning-Bog, C. Thiffault, J.W. Langston, D.A. Cory-Slechta, D.A. Di Monte, Neurobiol. Dis. 10 (2002) 119–127, http://dx.doi.org/10.1006/nbdi.2002.0507.
[23] T.I. Kam, X. Mao, H. Park, S.C. Chou, S.S. Karuppagounder, G.E. Umanah, S.P. Yun, S. Brahmachari, N. Panicker, R. Chen, S.A. Andrabi, C. Qi, G.G. Poirier, O. Pletnikova, J.C. Troncoso, L.M. Bekris, J.B. Leverenz, A. Pantelyat, H.S. Ko, L.S. Rosenthal, T.M. Dawson, V.L. Dawson, Science 362 (2018), http://dx.doi.org/10.1126/science.aat8407.
[24] H.T. Tran, C.H. Chung, M. Iba, B. Zhang, J.Q. Trojanowski, K.C. Luk, V.M. Lee, Cell Rep. 7 (2014) 2054–2065, http://dx.doi.org/10.1016/j.celrep.2014.05.033.
[25] K. Yanamandra, N. Kfoury, H. Jiang, T.E. Mahan, S. Ma, S.E. Maloney, D.F. Wozniak, M.I. Diamond, D.M. Holtzman, Neuron 80 (2013) 402–414, http://dx.doi.org/10.1016/j.neuron.2013.07.046.
[26] H. Asai, S. Ikezu, S. Tsunoda, M. Medalla, J. Luebke, T. Haydar, B. Wolozin, O. Butovsky, S. Kugler, T. Ikezu, Nat. Neurosci. 18 (2015) 1584–1593, http://dx.doi.org/10.1038/nn.4132.
[27] R. Shaltiel-Karyo, M. Frenkel-Pinter, N. Egoz-Matia, A. Frydman-Marom, D.E. Shalev, D. Segal, E. Gazit,PLoS One 5 (2010), e13863, http://dx.doi.org/10.1371/journal.pone.0013863.
[28] R. Gordon, E.A. Albornoz, D.C. Christie, M.R. Langley, V. Kumar, S. Mantovani, A.A.B. Robertson, M.S. Butler, D.B. Rowe, L.A. O'Neill, A.G. Kanthasamy, K. Schroder, M.A. Cooper, T.M. Woodruff, Sci. Transl. Med. 10 (2018), http://dx.doi.org/10.1126/scitranslmed.aah4066.
[29] X. Mao, M.T. Ou, S.S. Karuppagounder, T.I. Kam, X. Yin, Y. Xiong, P. Ge, G.E. Umanah, S. Brahmachari, J.H. Shin, H.C. Kang, J. Zhang, J. Xu, R. Chen, H. Park, S.A. Andrabi, S.U. Kang, R.A. Goncalves, Y. Liang, S. Zhang, C. Qi, S. Lam, J.A. Keiler, J. Tyson, D. Kim, N. Panicker, S.P. Yun, C.J. Workman, D.A. Vignali, V.L. Dawson, H.S. Ko, T.M. Dawson, Science 353 (2016), http://dx.doi.org/10.1126/science.aah3374.
[30] L.A. Volpicelli-Daley, K.C. Luk, T.P. Patel, S.A. Tanik, D.M. Riddle, A. Stieber, D.F. Meaney, J.Q. Trojanowski, V.M. Lee, Neuron 72 (2011) 57–71, http://dx.doi.org/10.1016/j.neuron.2011.08.033.
[31] S. Kim, S.H. Kwon, T.I. Kam, N. Panicker, S.S. Karuppagounder, S. Lee, J.H. Lee, W.R. Kim, M. Kook, C.A. Foss, C. Shen, H. Lee, S. Kulkarni, P.J. Pasricha, G. Lee, M.G. Pomper, V.L. Dawson, T.M. Dawson, H.S. Ko, Neuron (2019), http://dx.doi.org/10.1016/j.neuron.2019.05.035.
[32] D. Kim, J.M. Yoo, H. Hwang, J. Lee, S.H. Lee, S.P. Yun, M.J. Park, M. Lee, S. Choi, S.H. Kwon, S. Lee, S.H. Kwon, S. Kim, Y.J. Park, M. Kinoshita, Y.H. Lee, S. Shin, S.R. Paik, S.J. Lee, S. Lee, B.H. Hong, H.S. Ko, Nat. Nanotechnol. 13 (2018) 812–818, http://dx.doi.org/10.1038/s41565-018-0179-y.
[33] W. He, Y.T. Zhou, W.G. Wamer, X. Hu, X. Wu, Z. Zheng, M.D. Boudreau, J.J. Yin, Biomaterials 34 (2013) 765–773, http://dx.doi.org/10.1016/j.biomaterials.2012.10.010.
[34] C. Liu, Y. Yan, X. Zhang, Y. Mao, X. Ren, C. Hu, W. He, J. Yin, Nanoscale (2020), http://dx.doi.org/10.1039/C9NR10135G.
[35] W. He, Y. Liu, W.G. Wamer, J.J. Yin, J. Food Drug Anal. 22 (2014) 49–63, http://dx.doi.org/10.1016/j.jfda.2014.01.004.
[36] H. Fujiwara, M. Hasegawa, N. Dohmae, A. Kawashima, E. Masliah, M.S. Goldberg, J. Shen, K. Takio, T. Iwatsubo, Nat. Cell Biol. 4 (2002) 160–164, http://dx.doi.org/10.1038/ncb748.
[37] H.J. Kwon, D. Kim, K. Seo, Y.G. Kim, S.I. Han, T. Kang, M. Soh, T. Hyeon, Angew. Chem. Int. Ed. Engl. 57 (2018) 9408–9412, http://dx.doi.org/10.1002/anie.201805052.
[38] N. Singh, M.A. Savanur, S. Srivastava, P. D'Silva, G. Mugesh, Angew. Chem. Int. Ed. Engl. 56 (2017) 14267–14271, http://dx.doi.org/10.1002/anie.201708573.
[39] C. Hao, A. Qu, L. Xu, M. Sun, H. Zhang, C. Xu, H. Kuang, J. Am. Chem. Soc. 141 (2019) 1091–1099, http://dx.doi.org/10.1021/jacs.8b11856.
[40] D. Furtado, M. Bjornmalm, S. Ayton, A.I. Bush, K. Kempe, F. Caruso,Adv. Mater. 30 (2018), e1801362, http://dx.doi.org/10.1002/adma.201801362.
[41] G. Chandra, A. Roy, S.B. Rangasamy, K. Pahan, J. Immunol. 198 (2017) 4312–4326, http://dx.doi.org/10.4049/jimmunol.1700149.
[42] G. Halliday, M.T. Herrero, K. Murphy, H. McCann, F. Ros-Bernal, C. Barcia, H. Mori, F.J. Blesa, J.A. Obeso, Mov. Disord. 24 (2009) 1519–1523, http://dx.doi.org/10.1002/mds.22481.
[43] Y.B. Hu, E.B. Dammer, R.J. Ren, G. Wang, Transl. Neurodegener. 4 (2015) 18, http://dx.doi.org/10.1186/s40035-015-0041-1.
[44] X. Zhang, Y. Liu, S. Gopalakrishnan, L. Castellanos-Garcia, G. Li, M. Malassine, I. Uddin, R. Huang, D.C. Luther, R.W. Vachet, V.M. Rotello, ACS Nano 14 (2020) 4767–4773, http://dx.doi.org/10.1021/acsnano.0c00629.
[45] Y. Zhang, J. Hao, X. Xu, X. Chen, J. Wang, Anal. Chem. 92 (2020) 2080–2087, http://dx.doi.org/10.1021/acs.analchem.9b04593.
[46] Z. Zhang, M.L. Jorgensen, Z. Wang, J. Amagat, Y. Wang, Q. Li, M. Dong, M. Chen,Biomaterials 253 (2020), 120108, http://dx.doi.org/10.1016/j.biomaterials.2020.120108.
[47] M. Huo, L. Wang, Y. Wang, Y. Chen, J. Shi, ACS Nano 13 (2019) 2643–2653, http://dx.doi.org/10.1021/acsnano.9b00457.

[48] X. Mu, J. Wang, Y. Li, F. Xu, W. Long, L. Ouyang, H. Liu, Y. Jing, J. Wang, H. Dai, Q. Liu, Y. Sun, C. Liu, X.D. Zhang, ACS Nano 13 (2019) 1870–1884, http://dx.doi.org/10.1021/acsnano.8b08045.
[49] S. Zhao, H. Duan, Y. Yang, X. Yan, K. Fan, Nano Lett. 19 (2019) 8887–8895, http://dx.doi.org/10.1021/acs.nanolett.9b03774.
[50] H. Xiang, W. Feng, Y. Chen,Adv. Mater. 32 (2020), e1905994, http://dx.doi.org/10.1002/adma.201905994.
[51] H. Zhang, X.F. Lu, Z.-P. Wu, X.W.D. Lou, ACS Cent. Sci. (2020), http://dx.doi.org/10.1021/acscentsci.0c00512.